

Investigation of Pulsed Thermoelectric Performance by Impedance Spectroscopy

S. BOLDRINI ^{1,2}, A. FERRARIO,¹ and A. MIOZZO¹

1.—CNR – ICMATE, Corso Stati Uniti 4, Padua, Italy. 2.—e-mail: stefano.boldrini@cnr.it

A widespread use of thermoelectric technology usually collides with their limited efficiency. Efforts to overcome this limitation face difficulties in decoupling the thermal conductivity from the electrical conductivity (because of the Wiedeman–Franz law) and to obtain simultaneously high values of electrical conductivity and Seebeck coefficient (because of the Pisarenko relation). Some efforts to circumvent partially these limitations have been oriented to non-equilibrium solutions. These have been proved for cooling and in the last decade have been proposed as a means to increase power conversion from time varying thermal gradients. Another possibility that has been explored is the enhancement of thermal conversion efficiency obtained by periodically modulating the electronic load applied to a thermoelectric generator. Using impedance spectroscopy and pulsed loads applied to thermoelectric modules under adiabatic and non-adiabatic test conditions, we explored the role of several experimental parameters on the output power and conversion efficiency. We discuss operating limits and realistic perspectives of thermoelectric pulsed load application. Moreover, we examined the difference between air and vacuum impedance measurement for a thermoelectric module figure of merit determination and discussed the possible use of impedance spectroscopy as a tool for the study of thermal contact resistance by means of direct measurements under operating conditions.

Key words: Pulsed thermoelectric, impedance spectroscopy, conversion efficiency increase, thermal contact characterization

INTRODUCTION

Thermoelectricity is often considered as a candidate for the production of electricity through the recovery of thermal waste. In fact, it possesses many potentially interesting features, such as low costs, scalability, the possibility of being adapted to different temperature ranges, and relative simplicity in the design of thermoelectric generators. The absence of moving parts also results in low maintenance costs and the absence of noise emissions. Unfortunately, despite the improvements obtained in the two centuries of history of thermoelectric

phenomena, the conversion efficiency values are still rather limited. This limit has led to consider this technology as potentially interesting only for small applications,¹ for which the advantages listed above make it competitive with other technologies, notwithstanding the limited conversion efficiency.

Thermoelectric conversion efficiency is, under stationary conditions, the ratio of the electrical output power to adsorbed heat at the hot side. It thus depends on the product of the electrical conductivity and the square of the Seebeck coefficient and inversely from the thermal conductivity. Thermoelectrics evolution was limited by the coupling of electrical and thermal conductivity due to the Wiedeman–Franz law. A further limitation is posed by the inverse dependence on the carrier concentration of electrical conductivity and the

(Received August 23, 2018; accepted December 29, 2018; published online January 14, 2019)

Seebeck coefficient (described by the Pisarenko relation).

Among the various attempts to circumvent the obstacle, in the last two decades attention has been turned towards the possibility of exploiting solutions far from equilibrium. Pulsed-type solutions were initially proposed to increase the cooling performance of cryogenic systems based on the Peltier effect.²

Several attempts have been made to achieve improvements in conversion efficiency by using periodic heat sources or solutions that periodically interrupt the thermal contact between a thermoelectric generator (TEG) and heat source.^{3–6} Although coupling of TEGs with pulsed heat sources is to some extent effective in increasing conversion efficiency, this strategy has at least two major disadvantages. First, it requires overcoming constructional difficulties to adapt a TEG to a given heat source. This also eliminates a significant advantage of thermoelectric devices, i.e., the absence of moving parts. Second, an efficiency advantage is obtained for very high starting efficiencies and base operating regimes (those in stationary conditions) that are very far from the optimal ones. Generally, these improvements are obtained under constant flow operating conditions (with temperature values far from the maximum usable ranges) rather than for fixed temperature difference: this allows to increase the temperature on the hot side when they are used in alternating regime. This regime efficiency gain disappears when a device is employed under optimal conditions.

More recently, the possibility of increasing the conversion efficiency of a TEG simply by means of a dynamic load has been proposed. This load discontinuously absorbs power, while maintaining working temperatures or stationary input flows.⁷ A partial justification of this possible effect was found in the different internal resistance that is measured for a thermoelectric module as the frequency changes through impedance spectroscopy measurements.

Impedance spectroscopy (IS) allows in fact to collect numerous and interesting information about a material or a thermoelectric device. Originally proposed by Downey et al.⁸ for this purpose, it was later adopted in several works.^{9–15}

In these works, however, impedance spectroscopy is used under adiabatic conditions in order to obtain information on the properties of the thermoelectric modules or in the attempt to obtain measurements of the properties of the individual elements of thermoelectric material.

A difficulty encountered in the use of this technique lies in the definition itself of adiabatic conditions. In fact, if a module is characterized under vacuum, the contribution to heat flux produced by the air—normally present inside the module itself—is eliminated, resulting in overestimating its performance during typical module operation. On

the other hand, if the measurement is carried out in the air, it is the exchange on the external faces of the module that add a parasitic heat flux contribution.¹⁶ In this paper we have therefore analysed different solutions in terms of thermal effusivity and we propose a comparison between impedance spectroscopy measurements carried out in vacuum, in air and with the thermoelectric module enclosed between two plates of expanded polystyrene (EPS) or silica aerogel.

In adiabatic conditions, impedance measurement on a thermoelectric module in Nyquist representation results in a semicircle at low frequencies, typical of an RC circuit. The resistance and capacity values, in addition to the time constant τ given by their product, have been related to the thermoelectric parameters of the module, to its dimensions and to the thermal diffusivity of the used materials. In particular, the apparent resistance value is proportional to the Seebeck and Peltier product and the thickness of the module and inversely to its surface and thermal conductivity. Since this resistance value, which is substantially the difference between a high frequency and a DC electrical resistance measurement, typically is of the same order of magnitude as the internal resistance, one might be led to think that operating with a high dynamic load frequency can significantly increase the electric power and consequently the efficiency.⁷

In this paper we also report impedance spectroscopy measurements performed on modules under realistic operating conditions, i.e., between two temperature values, and we show—to the best of our knowledge for the first time—how these conditions give rise to a significantly different behaviour and unfortunately less promising from the point of view of an increase in efficiency.

Finally some tests performed with square waves of different period and duty cycle reveal the difference between the single (or few) wave used for impedance measurement and the real periodic pulsed operation.

EXPERIMENTAL

Impedance spectroscopy measurements were collected using a Ref 600 (Gamry instrument) from several different thermoelectric modules, connected in the four-wire configuration with connections as close as possible to the module. Frequency was normally varied from 10 kHz down to few mHz, depending on the possibility to maintain stable conditions for long time, collecting 10 log-spaced frequency points per decade. In some cases frequencies up to 1 MHz were tested, resulting in inductive effects. Modules ranged from 4 mm × 4 mm up to 62 mm × 62 mm. Modules were tested both in adiabatic (vacuum, $\approx 10^{-3}$ mbar) or *semi*-adiabatic (air, expanded polystyrene, silica aerogel) conditions and under realistic operating conditions.

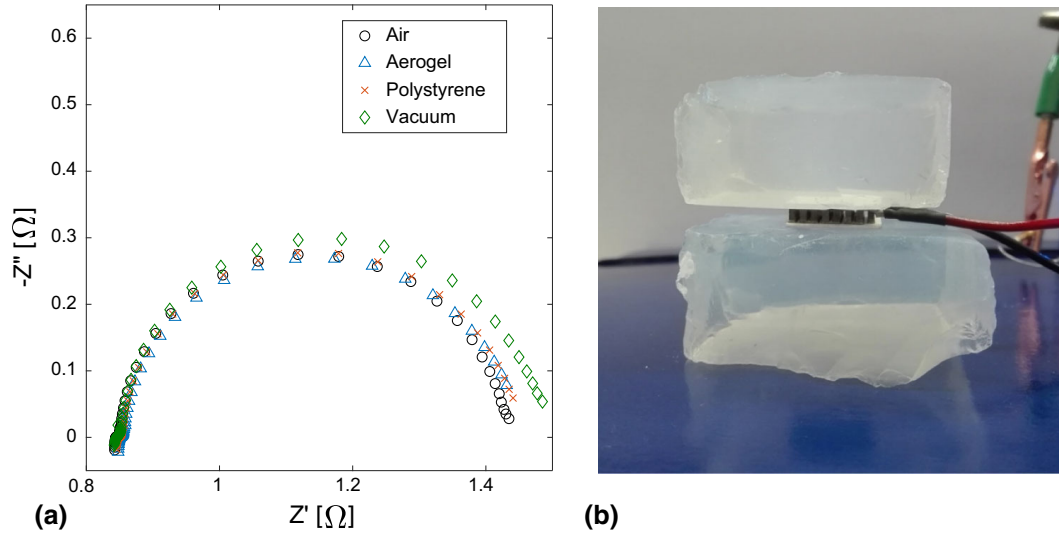


Fig. 1. (a) Nyquist representation of impedance measurement obtained in vacuum, air and sandwiched between two large silica aerogel or EPS slabs, (b).

During adiabatic tests, realized both in galvanostatic (not reported here) and potentiostatic mode, signals of about 50 mVrms (potentiostatic) without any DC component were used.

Operating conditions tests were performed employing a home built test station (not described here). Thermoelectric modules are placed between two metallic blocks (copper for the hot side, aluminium alloy for the cold side) with a controlled pressure. Hot (T_H) and cold (T_C) side temperatures are controlled, and the heat flux at the cold side is measured by means of a thermocouple array and suitable calibrations. The time constant for the heat flow measurements is about 1 s. Different thermal interface materials and applied pressures were used to evaluate the effect of good or poor thermal contacts. To simulate an active load, which opens and closes a circuit on a matched load (for maximum power), impedance spectroscopy measurements were obtained with potentiostatic mode, using sinusoidal signals ranging from open circuit potential (V_{OC}) to half open circuit potential. This corresponds to currents oscillating from 0 A to the half of a short circuit current. This choice was also motivated by the possibility of easily comparing impedance spectroscopy measurement with maximum power matched conditions.

Finally, for square wave pulsed tests, a source meter unit (Keithley 2601B) was used as electronic load. Current pulse trains (2 min long) were applied, with 2 ms to 20 ms pulse period and 10% to 90% duty cycle (inset in Fig. 6). Tests were performed both for good and poor thermal coupling. The current applied during each pulse has been set in order to obtain, after a long pulse train (at equilibrium), a potential equal to the half of V_{OC} .

Table I. results of the fit of Fig. 1 Nyquist data: ZT values obtained from Eq. 1

	R_{HF} (Ω)	R_{TE} (Ω)	C_{TE} (F)	ZT
Air	0.845	0.567	12.1	0.67
Silica aerogel	0.845	0.562	12.8	0.66
EPS	0.849	0.574	12.3	0.68
Vacuum	0.845	0.613	12.1	0.73

RESULTS AND DISCUSSION

Adiabatic Test

Impedance tests are normally performed under vacuum, in order to suppress at least thermal conduction and convection in the module surrounding air, which has been proved to be an error source¹⁶ for these measurements. Some parameters could be obtained from the impedance diagram fit. Among them the high frequency resistance, R_{HF} (i.e., the electrical internal resistance R_{Ω} , the left-most intersection of data with the real axis in Fig. 1, or the series resistance in the equivalent circuit), and the thermoelectric resistance R_{TE} (the resistance associated with the RC equivalent circuit) allow to estimate the figure of merit as¹⁵

$$ZT = \frac{R_{TE}}{R_{HF}} \quad (1)$$

Unfortunately, measuring under vacuum could produce an overestimation of the apparent conversion efficiency achievable under normal module operation (at atmospheric pressure). Neglecting the convection in the air inside the module, the

thermoelectric material and air conductance ratio could be expressed as:

$$\frac{K_{TE}}{K_{air}} = \frac{\lambda_{TE}}{\lambda_{air}} \cdot \frac{f}{1-f}, \quad (2)$$

where f is the module fill factor and λ the thermal conductivity of thermoelectric device and air. Considering them as typical values for a commercial module: $\lambda_{TE} = 1.5$ W/mK, $\lambda_{air} = 0.03$ W/mK and $f = 0.3$, the parasitic contribution to heat flux produced by air conduction is about 5% of the total.

Figure 1 shows the impedance measurements obtained at room temperature for a 20 mm × 20 mm module (31 couples) in vacuum (10^{-3} mbar), in air, and obtained by placing the module between two slabs (5 cm side, thickness of 2 cm) of silica aerogel or EPS. The latter configuration was chosen in order to suppress external air convection while maintaining air conduction in the thermoelectric module gaps. For silica aerogel the estimated time for heat to go through the plate is about 7 min: for frequencies down to a few mHz it can reasonably be considered a semi-infinite plate. The thermal perturbation produced by the insulating layer could be neglected.* We note that measurements made in air and with insulating materials result in closer values, with lower R_{TE} . The figure of merit ZT obtained with Eq. 1, and reported in Table I, resulted in being the same for the air, silica aerogel and EPS measurement, but significantly higher for the vacuum one (7–10% higher). This ZT difference can be attributed to the reduction in thermal difference produced by air conduction inside the module. It is worth noting that if heat removal by conduction in insulating materials were higher than the heat removed by external air (both conduction and convection), this would result in a lower ZT value for these measurements, if compared with air measurement. For this reason, adequately insulating a thermoelectric module (e.g., with silica aerogel or EPS) and measuring at room pressure seem to be the most appropriate technique to obtain a reliable value of the module effective ZT .

Furthermore, vacuum measurement requires careful design in order to minimize Joule heating. Employing large signal (e.g., 100 mVrms) in order to reduce measurement noise could easily result in a few degrees temperature increase during an impedance measurement: since frequency scans normally start from higher frequency, this in turn results in an additional small overestimation of ZT .

Operating Condition Measurements

The apparently large difference between DC and high frequency electrical resistance (see Fig. 1a) is among the reasons⁷ used to motivate the possible

*The thermal effusivity ($e = (\lambda\rho c_p)^{0.5}$) of air and insulating material were similar and < 0.5% of Al_2O_3 effusivity.

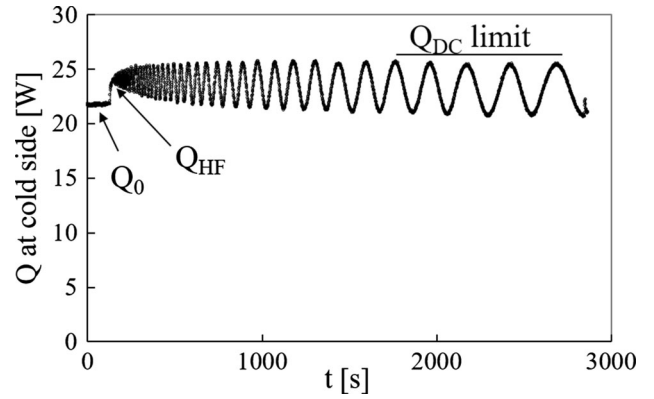


Fig. 2. Heat flux measured at cold side during an impedance spectroscopy scan from 10 kHz to a few mHz.

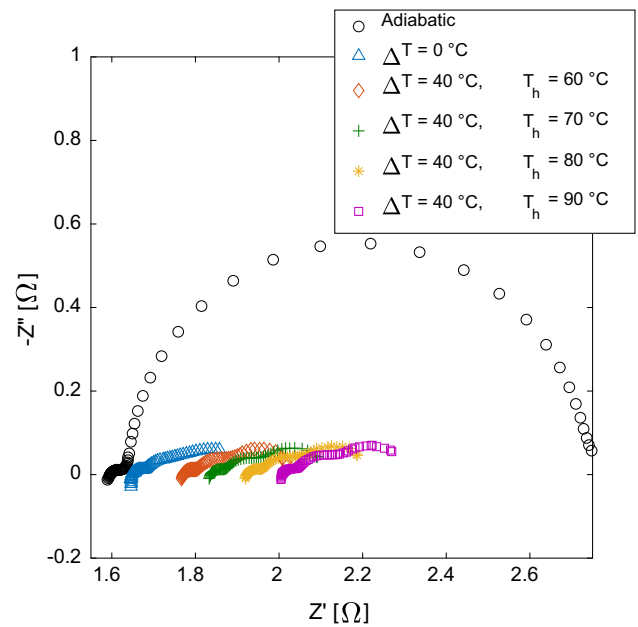


Fig. 3. Nyquist representation of impedance measurements obtained under adiabatic or operating condition (i.e., in thermal contact with a hot source and a heat sink).

advantage produced by pulsed operation. This could apparently result from the electrical power increase produced by a lower internal resistance,

$$P = V_{OC}^2 \cdot \frac{R_{load}}{(R_{load} + R_i)^2}, \quad (3)$$

where R_{load} is the load resistance and R_i the module internal resistance, combined with the thermal flux reduction. The latter results from the intermittent nature of the current dependent contribution to heat flux (neglecting the Thomson effect):

$$Q = K \cdot \Delta T + I\alpha T_H - \frac{1}{2}R_i I^2 = Q_0 + C(I). \quad (4)$$

With K (K/W) the thermal conductance of the module, $\alpha = N(\alpha_p - \alpha_n)$ the Seebeck coefficient for N

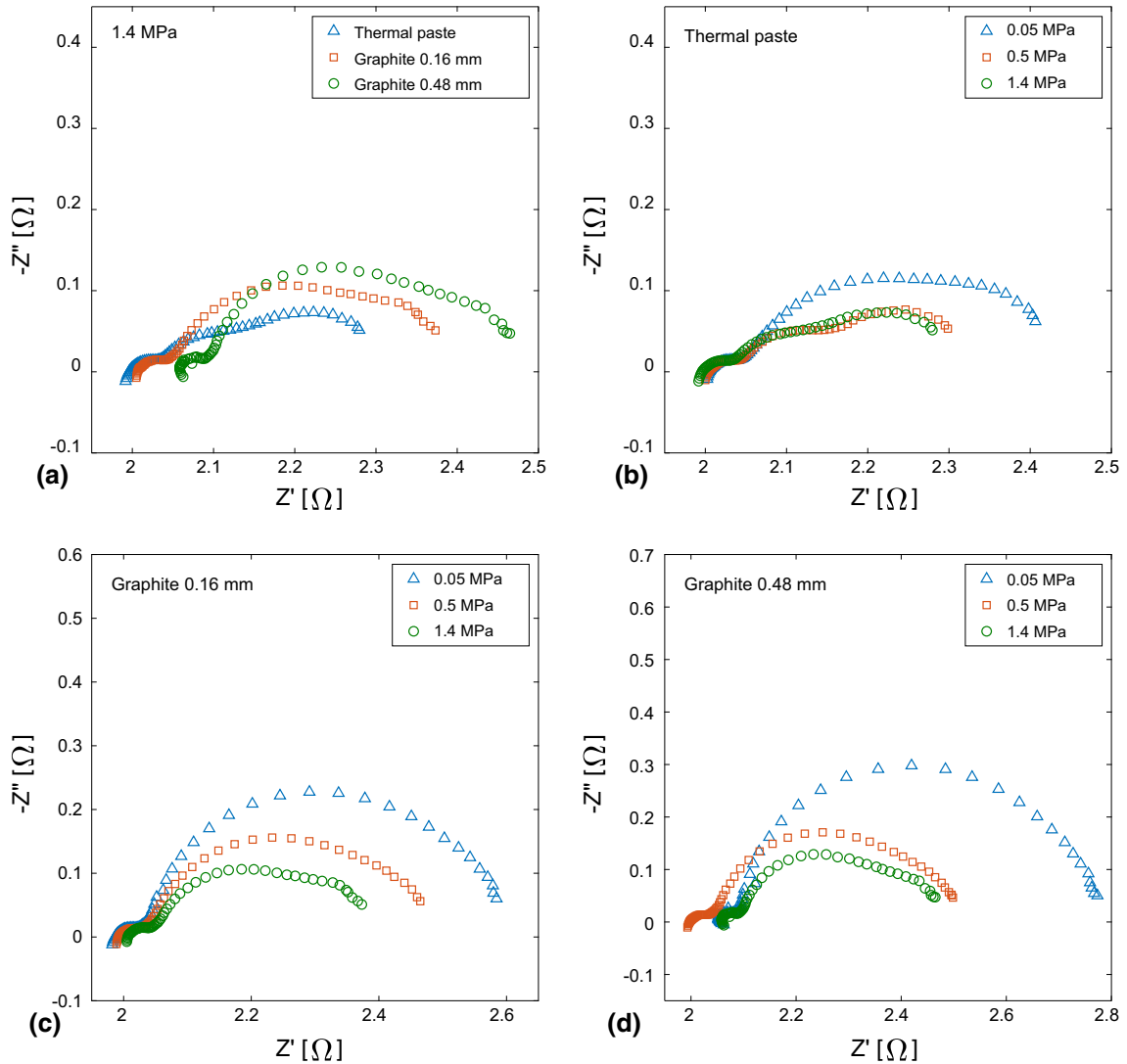


Fig. 4. (a) Impedance data collected with different interface materials at 1.4 MPa, $T_H = 90^\circ\text{C}$ and $T_C = 50^\circ\text{C}$. Impedance data comparison at three different applied pressures (0.05 MPa, 0.5 MPa and 1.4 MPa) for (b) thermal paste, (c) 0.16 mm and (d) 0.48 mm.

couples and T_H the hot side temperature. $C(I)$ is the current dependent heat flux, and since the Joule contribution is small if compared to the Peltier, $C(I)$ is with good approximation proportional to I . Figure 2 shows the typical heat flux measured at the cold side during a frequency scan (from high to low frequency) in an impedance measurement.

The last term in Eq. 4 is affected by a pulsed operation (even if the hot and cold side temperatures remain constant). Being D the duty cycle:

$$Q_{\text{HF}} \approx Q_0 + D \cdot C(I). \quad (5)$$

R_{TE} results proportional to $T_H - T_C$,¹² but this temperature difference is produced by the equilibrium of the Peltier thermal flux, resulting in a temperature gradient in the material, and the Fourier thermal flux. Temperature difference tends to be

drastically lower when the module is no longer in adiabatic conditions and the same happens to R_{TE} . Figure 3 reports the impedance data collected on a $40 \text{ mm} \times 40 \text{ mm}$ thermoelectric module (TG 12-8, II-VI Marlow) in adiabatic conditions, clamped between two metallic slabs (Cu and Al alloy) at room temperature using thermal paste and 1.4 MPa, and applying temperature differences. Clearly, the coupling between thermoelectric module and metallic slabs reduces the low frequency impedance: the heat transfer to the metal reduces the thermal gradient inside the module and consequently the Harman over-potential. In the limit case, where the module is in contact with two thermal reservoirs, the temperature difference within the thermoelectric material, produced by applied current during impedance measurement, would equal the temperature difference across a module passive element (ceramic and

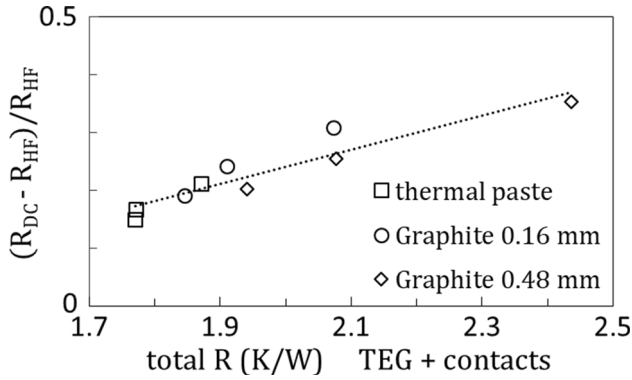


Fig. 5. Impedance results as a function of total thermal resistance (thermoelectric module + different interface materials and applied contact pressures).

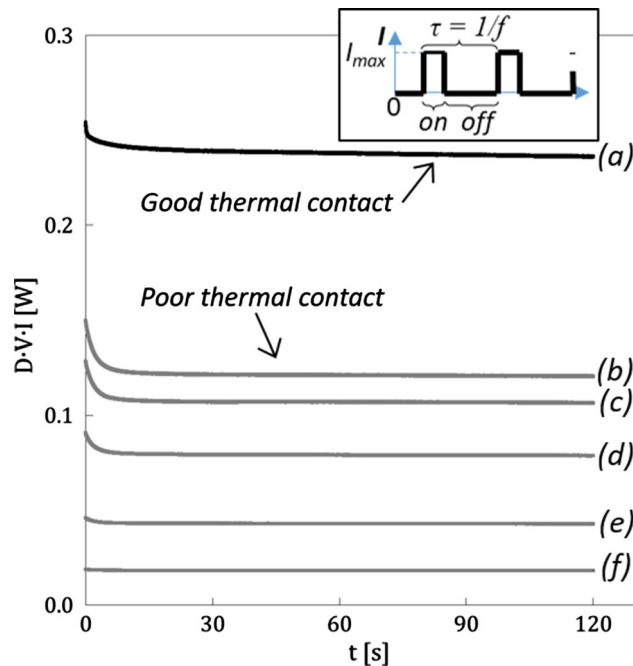


Fig. 6. Output power recorded with a square wave load, $T_H = 90^\circ\text{C}$ and $T_C = 50^\circ\text{C}$, for different values of the applied duty cycle. Data were recorded either with a good thermal contact (thermal paste, 1.4 MPa), using a 50% duty cycle and 487 mA (a) or with poor thermal contact (0.48 mm graphite and 0.05 Mpa) for: $D = 0.9$ and 225 mA (b), $D = 0.75$ and 237 mA (c), $D = 0.5$ and 261 mA (d), $D = 0.25$ and 283 mA (e) and $D = 0.1$ and 299 mA (f).

contact resistances), with opposite sign. For this reason, impedance measurements allow to evaluate variations in the thermal resistance in the coupling of a module with heat source and heat sink.

To study the effect of contact resistance, the same module was tested (between $T_H = 90^\circ\text{C}$ and $T_C = 50^\circ\text{C}$) varying the applied pressure (0.05 MPa, 0.5 MPa and 1.4 MPa) and the interface material

(thermal paste, one or three 0.16 mm thick graphite foils). Thermal paste and 1.4 MPa pressure are the condition recommended by the manufacturer. Figure 4 shows the impedance data obtained with $T_H = 90^\circ\text{C}$ and $T_C = 50^\circ\text{C}$, for different values of interface thermal resistance, obtained varying the interface material, thickness and pressure. Worsening the thermal contact increases the low frequency impedance.

Figure 5 shows the relative electrical resistance difference $(R_{DC} - R_{HF})/R_{HF}$, where R_{DC} is the low frequency limit (obtained from the fit) and R_{HF} the high frequency resistance, versus the measured thermal resistance of TE module and interfaces materials. The latter is measured under open circuit conditions as the ratio of $\Delta T = T_H - T_C$ and the heat flux measured at the cold side. Different thermal resistance values correspond to the three different applied pressures. Since this electrical parameter increases with total thermal resistance, it appears that impedance measurements can be profitably used to study/monitor thermal interface resistances, even without the need for temperature measurements. Impedance spectroscopy allows developing suitable procedures, based only on electrical measurements on the TE module, to test contact resistance dependence from interface nature, contact pressure or other parameters in a thermoelectric generator.

Pulsed Operation

Even if impedance spectroscopy revealed a powerful technique, moving from its results to the pulsed operation is not straightforward. In fact, impedance data are usually collected using one or few wave periods, while in pulsed operation the heat flux tends to cumulate. In Fig. 6 we report the maximum output power recorded with different duty cycles. In a 2 ms long period the load applied was I_{max} for a fraction D (duty cycle) of the period and zero (open circuit) for the remaining time. During current application, voltage was measured, in order to calculate power output. These power outputs are average values, corrected for the duty cycle. At these frequencies, around 1 kHz, there is no phase shift between current and voltage, as revealed by the impedance measurements. Part of the output power gain produced by the apparently lower internal resistance at high frequency disappears after a few seconds. As D increases, the difference between first pulse and the power after some seconds also increases. This could result from the higher heat flux for higher D (Eq. 5). For good thermal contact, obviously, higher output power was found (due to the higher actual temperature gradient in the module). After a few seconds, power converged to about 0.235 W. On the same thermoelectric module, we measured a steady state

maximum power of 0.47 W in the same conditions, about the double of the power registered with a 50% duty cycle.

CONCLUSIONS

In the last decade, impedance spectroscopy attracted increasing attention as a tool for the study of thermoelectric devices and materials. One of the most consolidated applications is the determination of the figure of merit of thermoelectric devices. In this work we propose to improve its accuracy by testing directly at room pressure, suppressing possible convection losses with suitable thermal insulators. Furthermore, we used impedance measurement to investigate the possibility of taking advantage of a pulsed operation of thermoelectric devices. We performed some preliminary tests of thermoelectric modules under realistic operating conditions, as far as we known not previously reported in the literature. We outlined also the possibility to use impedance spectroscopy to study or monitor interface contact resistance of thermoelectric devices without the need for temperature measurements. The supposed gain in internal resistance at high frequency, if compared to steady state operation, was shown to slowly vanish as the thermal coupling with a heat source and a heat sink is improved. Directly testing thermoelectric

modules with square wave load at high frequencies also supported these observations.

REFERENCES

1. C.B. Vining, *Nat. Mater.* 8, 83 (2009).
2. G.J. Snyder, J.P. Fleurial, T. Caillat, R. Yang, and G. Chen, *J. Appl. Phys.* 92, 1564 (2002).
3. Y. Yan and J.A. Malen, *Energy Environ. Sci.* 6, 1267 (2013).
4. O. Yamahsita, H. Odahara, and K. Satou, *J. Appl. Phys.* 101, 023704 (2007).
5. G. Min, *AIP Conf. Proc.* 1449, 447 (2012).
6. I.S. McKay and E.N. Wang, Thermal pulse energy harvesting. *Energy* 57, 632 (2013).
7. J.G. Stockholm, C. Goupil, P. Maussion, and H. Ouerdane, *J. Electron. Mater.* 44, 1768 (2015).
8. A.D. Downey, T.P. Hogan, and B. Cook, *Rev. Sci. Instrum.* 78, 093904 (2007).
9. A. De Marchi and V. Giaretto, *Rev. Sci. Instrum.* 82, 034901 (2011).
10. A. De Marchi and V. Giaretto, *Rev. Sci. Instrum.* 82, 104904 (2011).
11. A. De Marchi, V. Giaretto, S. Caron, and A. Tona, *J. Electron. Mater.* 42, 2067 (2013).
12. J. García-Cañadas and G. Min, *J. Electron. Mater.* 43, 2411 (2014).
13. J. García-Cañadas and G. Min, *J. Appl. Phys.* 116, 174510 (2014).
14. J. García-Cañadas and G. Min, *AIP Adv.* 6, 035008 (2016).
15. B. Beltrán-Pitarch, J. Prado-Gonjal, A.V. Powell, P. Ziolkowsky, and J. García-Cañadas, *J. Appl. Phys.* 124, 025105 (2018).
16. B. Beltrán-Pitarch and J. García-Cañadas, *J. Appl. Phys.* 123, 084505 (2018).